Visualizing the itch-sensing skin arbors

Yanyan Xing[1], **Haley R. Steele**[1], **Henry B. Hilley**, **Yuyan Zhu**, **Katy Lawson**, **Taylor Niehoff**, **Liang Han**[*]

School of Biological Sciences, Georgia Institute of Technology, Atlanta, GA, United States

Abstract

Diverse sensory neurons exhibit distinct neuronal morphologies with a variety of axon terminal arborizations subserving their functions. Due to its clinical significance, the molecular and cellular mechanisms of itch are being intensely studied. However, a complete analysis of itch-sensing terminal arborization is missing. Using a *MrgprC11^CreERT2^* transgenic mouse line, we labeled a small subset of itch-sensing neurons that express multiple itch-related molecules including MrgprA3, MrgprC11, histamine receptor H1, IL-31 receptor, 5-HT receptor 1F, natriuretic precursor peptide B, and neuromedin B. By combining sparse genetic labeling and whole-mount PLAP histochemistry, we found that itch-sensing skin arbors exhibit free endings with extensive axonal branching in the superficial epidermis and large receptive fields. These results revealed the unique morphological characteristics of itch-sensing neurons and provide intriguing insights into the basic mechanisms of itch transmission.

INTRODUCTION

Primary somatosensory neurons detect nociception, mechanical stimulation, and body location via peripheral axons, located in both the skin and visceral organs, and transmit signals to the spinal cord via central axons. Diverse sensory neurons are classified by molecular composition, neurophysiological properties (axon diameter, myelination, and conduction velocity), and defined functions. This diversity is also evidenced by distinct innervation patterns involving the morphology of peripheral and central axon terminal arborizations, specialized peripheral anatomical structures associated, termination zones within particular lamina of the spinal cord dorsal horn, and somatotopic organization

DATA AVAILABILITY STATEMENT

No datasets were generated or analyzed during the current study.

CONFLICT OF INTEREST

The authors claim no conflict of interest.

(Abraira and Ginty, 2013, Basbaum et al., 2009, Crawford and Caterina, 2020, Ikoma et al., 2006). For example, most cutaneous mechanosensors innervate hair follicles and skin end organs, such as Merkel cells and Meissner corpuscle, and project central axons to the laminar III-V of the spinal cord dorsal horn (Abraira and Ginty, 2013). In contrast, nociceptors mediating pain and itch innervate the epidermis as free nerve endings and their central axons terminate within the outermost lamina of the dorsal horn (lamina I and II) (Han et al., 2013, Zylka et al., 2005). Thus, morphological and anatomical analysis of sensory innervation patterns is fundamental to understand somatosensory processing. Indeed, deep functional insights on touch sensation and sensory acuity were revealed from the integration of morphological and physiological characterizations of several subtypes of sensory neurons including the low-threshold mechanoreceptors (LTMRs) and non-peptidergic nociceptors (Bai et al., 2015, Ghitani et al., 2017, Kuehn et al., 2019, Li and Ginty, 2014, Li et al., 2011, Olson et al., 2017, Rutlin et al., 2014).

Itch, a somatosensory modality mainly arising from the skin, serves as an alert to potential threats. However, chronic itch associated with dermatological and systemic disorders is a debilitating symptom that is often refractory to available treatments (Ikoma et al., 2006). Three distinct itch-sensing neuronal populations were previously identified by their unique combination of itch receptors: MrgprA3+ neurons are enriched with MrgprC11 and histamine receptors (Han et al., 2013, Liu et al., 2009, Sharif et al., 2020, Sharma et al., 2020, Xing et al., 2020); Nppb+ neurons express receptors for IL31 (Il31ra), cysteinyl leukotriene (Cysltr2), serotonin (Htr1f), and sphingosine-1-phosphate (S1pr1) (Solinski et al., 2019); and MrgprD+ neurons express lysophosphatidic acid receptors (Lpar3 and Lpar5) (Liu et al., 2012, Sharma et al., 2020, Usoskin et al., 2015). While recent investigations have given us a glimpse of the molecular, cellular, and circuitry basis of itch processing, analysis of the itch-sensing terminal arborization is missing.

In the present study, by combining spare genetic labeling and whole-mount PLAP histochemistry staining, we successfully trace the morphology of a subset of itch-sensing neurons. These neurons are mainly peptidergic and express multiple itch-related molecules including MrgprA3, MrgprC11, IL31ra, Hrh1, Htr1f, Nppb, and Nmb. Peripheral itch-sensing arbors in the skin are characterized by free endings with extensive axonal branching in the superficial epidermis. Their arbor areas are much larger than the MrgprB4+ and MrgprD+ arbors, suggesting that itch-sensing neurons have large receptive fields. These results reveal the unique morphology of itch-sensing arbors and help us to understand how itch is initiated in the skin.

RESULTS

MrgprC11^CreERT2 leaky neurons label a small subset of peptidergic nociceptors.

MrgprC11 is a recently identified itch receptor in the Mas-related G protein-couple receptor (Mrgpr) family. It is specifically expressed in small-diameter DRG sensory neurons with several identified pruritogen agonists including Bam8–22, SLIGRL, and Cathepsin S (Liu et al., 2009, Liu et al., 2011, Reddy et al., 2015). To investigate the morphological characteristics of itch-sensing neurons, we generated a BAC (bacterial artificial chromosome) transgenic *MrgprC11^CreERT2* mouse line (Figure 1A) and utilized the

tamoxifen-inducible CreERT2/loxP system to perform sparse genetic labeling and neuronal morphology tracing. Using our previously validated MrgprC11 antibody (Han et al., 2018), we detected the expression of MrgprC11 in $17.2 \pm 1.1\%$ (n = 3 mice) of DRG sensory neurons (Figure 1B). Interestingly MrgprA3$^+$ neurons are a subpopulation of MrgprC11$^+$ neurons (Figure 1B), highlighting the significant role of MrgprC11$^+$ neurons in itch transmission. We have crossed the *MrgprC11*^{CreERT2} mice with Cre-dependent *Rosa26*^{tdTomato} line to label MrgprC11$^+$ neurons with tdTomato fluorescence. After tamoxifen treatment to activate CreERT2, $91.6 \pm 0.5\%$ of MrgprC11$^+$ neurons express tdTomato$^+$ and $95.7 \pm 1.0\%$ (n = 3 mice) of the tdTomato$^+$ neurons exhibit the MrgprC11 immunoreactivity (Figure 1C). These results suggest that the expression of CreERT2 is tightly controlled by the endogenous MrgprC11 promoter.

We found sparse recombination in $0.96 \pm 0.3\%$ of DRG sensory neurons (n = 3 mice, referred to as MrgprC11^{CreERT2} leaky cells) in the absence of tamoxifen treatment (Figure 1D and E). This leaky Cre activity is often observed in CreERT2 lines (Hans et al., 2009, Hooijkaas et al., 2012, Olson et al., 2017, Stone et al., 2018). Detailed morphological and anatomical analysis of sensory neurons requires visualization of single sensory arbors, which is technically challenging because sensory arbors always overlap and intermingle. This leaky CreERT2 activity provides a tool for sparse genetic labeling and may allow us to visualize non-overlapping individual arbors. Therefore, we first examined the molecular feature of MrgprC11^{CreERT2} leaky cells to see if they represent itch-sensing neurons. We confirmed the expression of MrgprC11 in these neurons using both immunostaining with a MrgprC11 antibody (Figure 1D) and *in situ* hybridization (Figure 1E). Immunostaining showed that $89.1 \pm 7.4\%$ of MrgprC11^{CreERT2} leaky cells are recognized by the MrgprC11 antibody. Similarly, *in situ* hybridization analysis demonstrated that $84.6 \pm 1.6\%$ of MrgprC11^{CreERT2} leaky cells express MrgprC11. These MrgprC11^{CreERT2} leaky cells represent about 5.6% of the whole MrgprC11$^+$ neuronal population.

These MrgprC11^{CreERT2} leaky cells are small diameter ($260.11 \pm 14.82 \ \mu m^2$) neurons, positive for the nociceptive marker TRPV1 (85.9%, Figure 2A), and the peptidergic marker substance P (86.0%, Figure 2B), and negative for myelinated neuron marker neurofilament 200kD (NF200, Figure 2F). A subset were positive for peptidergic marker calcitonin gene-related peptide (CGRP, Figure 2C), the nonpeptidergic nociceptive marker IB4 (Figure 2D), and the purinergic receptor X3 (P2X3, Figure 2E). Moreover, these neurons are distinct from the MrgprB4$^+$ neurons (Figure 2G) whose arbor morphology were previously revealed (Liu et al., 2007). Therefore, MrgprC11^{CreERT2} leaky neurons are a small subset of peptidergic nociceptors.

MrgprC11^{CreERT2} leaky neurons represent itch-sensing neurons expressing multiple itch receptors

Surprisingly, MrgprC11^{CreERT2} leaky cells expressed multiple itch-related molecules including MrgprA3 (66%, Figure 3A) and Nppb (70%, Figure 3C), markers for two distinct itch-sensing subtypes (Han et al., 2013, Sharma et al., 2020, Solinski et al., 2019, Usoskin et al., 2015). The majority of neurons expressed histamine receptor (Hrh1, 72.2%, Figure 3B), which are enriched in MrgprA3$^+$ neurons. They were also positive for Il31ra (75.7%, Figure

3D) and Htrf1 (56.3%, Figure 3E), which are enriched in Nppb$^+$ neurons. Moreover, 63.1% of them expressed neuromedin B (Nmb, Figure 2F), a neuropeptide required for histaminergic itch (Wan et al., 2017). Very few of them expressed MrgprD or Lpar3 (0.9% and 0.9% respectively, Figure 3G–H), markers for MrgprD$^+$ itch-sensing neurons. The expression of multiple itch-related molecules in MrgprC11^{CreERT2} leaky cells indicates that they are itch-sensing neurons.

We next performed calcium imaging with cultured dissociated neurons to examine if they exhibit neuronal responses to pruritogens. We generated *MrgprC11^{tdTomato}; Pirt^{GCaMP3}* mice that express the calcium indicator GCaMP3 in all sensory neurons (Kim Y. S. et al., 2014). MrgprC11^{CreERT2} leaky cells were labeled by tdTomato fluorescence. Consistent with the expression of itch receptors, most MrgprC11^{CreERT2} leaky neurons responded to MrgprA3 agonist chloroquine (90.3%), MrgprC11 agonist Bam8–22 (91.1%), histamine (87.7%), IL-31 (85.1%), and 5-HT1F receptor agonist LY344864 (68.4%). Almost all cells also responded to the TRPV1 agonist capsaicin (98.0%) (Figure 4A–B and 4D). None of the tested cells responded to the application of MrgprD agonist β-alanine or LPA (Figure 4C–D).

We then employed a chemogenetic approach to examine if activation of MrgprC11^{CreERT2} leaky cells can induce itch behavior in mice. We generated *MrgprC11^{DREADD}* mice by crossing our *MrgprC11^{CreERT2}* line with the *Rosa26^{DREADD}* line. Immunohistochemistry analysis confirmed the expression of Dreadd in MrgprC11$^+$ neurons (Figure 4E). Subcutaneous injection of CNO into the nape of the neck skin induced robust scratching behaviors in *MrgprC11^{DREADD}* mice, but not in *Rosa26^{DREADD}* control mice (Figure 4F). This data indicates that the activation of MrgprC11^{CreERT2} leaky neurons induces itch sensation. In summary, these data suggest that MrgprC11^{CreERT2} leaky neurons, which constitute approximately 1% of DRG sensory neurons, represent itch-sensing neurons. Our *MrgprC11^{CreERT2}* line provides a genetic tool for sparse genetic tracing to investigate the morphological features of itch-sensing neurons.

Itch-sensing skin arbors are characterized by free endings with extensive axonal branching in the superficial epidermis and large receptive fields

We crossed the *MrgprC11^{CreERT2}* mice with Cre-dependent *Rosa26^{IAP}* line to express the axonal tracer PLAP (human placental alkaline phosphatase) in MrgprC11^{CreERT2} leaky cells. We observed 41–102 PLAP$^+$ neurons/DRG (53.4 ± 3.6 neurons/cervical DRG, 64.2 ± 3.4 neurons/thoracic DRG and 79 ± 3.6 neurons/lumbar DRG) (Figure 5A). Their central arbors in the spinal cord dorsal horn exhibit rostrocaudal elongation and mediolateral compression (Figure 5B), which is consistent with the previous examined C-type arbors from Golgi staining or single-cell tracer filling (Scheibel and Scheibel, 1968, Sugiura et al., 1986, Sugiura et al., 1989). Except for the central sensory arbors, we did not observe PLAP signals in any spinal neurons, consistent with the fact that MrgprC11 is mainly expressed in sensory neurons (Han et al., 2018).

Their peripheral arbors in the skin cover ~80% of the skin surface area. The arbor density increased proximally and in the upper part of the body (Figure 5C). Arbors were observed in the distal limbs, but only the dorsal skin of the paws. Although MrgprC11$^+$ neurons, when

examined as a whole population (Han et al., 2013), do innervate glabrous skin, MrgprC11^{CreERT2} leaky cells arbors were not observed in the plantar glabrous skin (Figure 5D). Most of the skin arbors are overlapping and do not allow analysis of individual arbors. Only non-overlapping arbors were selected for morphological analysis. The morphology of MrgprC11$^+$ arbors in the skin is consistent among animals, and are typical arbors with "free endings" featuring extensive axonal branching uniformly covering the whole area (Figure 5E). These features indicate that the axon terminals are free nerve endings in the superficial epidermis. Circumferential-like endings associated with hair follicles were occasionally observed (Figure 5E) in approximately 10% of the arbors. We then used tamoxifen-treated *MrgprC11^{tdTomato}* mice to label all MrgprC11$^+$ neurons with tdtomato fluorescence and confirmed this innervation pattern in skin sections. We observed tdTomato$^+$ skin nerves penetrate to the most superficial skin layer (Figure 5G), a feature typical of itch-sensing nerves (Han et al., 2013). We occasionally observed circumferential endings with tdTomato$^+$ nerves wrapping around hairy follicles (Figure 5G). We did not observe any tdTomato signals in skin residential cells.

Itch-sensing skin arbors exhibit large receptive fields

We compared the morphology of itch-sensing skin arbors with MrgprD^{CreERT2} leaky neurons and MrgprB4$^+$ neurons (Figure 5E). MrgprD^{CreERT2} leaky neurons represent non-peptidergic nociceptors whose arbor morphology was revealed by the background recombination of *MrgprD^{CreERT2}* line (Olson et al., 2017, Olson and Luo, 2018). Consistent with the previous report, we found that these arbors have "bushy ending" morphology, featuring dense and finely branched processes and clustered terminal neurites. Their axons show both free nerve endings in the epidermis and frequent circumferential endings (Figure 5E). MrgprB4$^+$ neurons, which constitute about 2% of DRG sensory neurons, are mechanosensory C-fibre mediating pleasant stroking of hairy skin. Their skin arbors also exhibit free ending morphology visualized using *MrgprB4^{PLAP}* knockin mouse line (Figure 5E) (Liu et al., 2007). Arbor areas were significantly different, with MrgprC11^{CreERT2} leaky neurons showing the largest arbor area and MrgprD^{CreERT2} leaky neurons showing the smallest. Only non-overlapping MrgprC11$^+$ arbors in the trunk skin and dorsal hindpaw skin were selected for quantification. The size difference is more prominent in the dorsal hindpaw skin with the size of MrgprC11$^+$ arbors triple the size of the other two subtypes (1.60 ± 0.08 mm^2 for MrgprC11^{CreERT2} leaky neurons, 0.55 ± 0.03 mm^2 for MrgprB4$^+$ neurons, 0.37 ± 0.02 mm^2 for MrgprD^{CreERT2} leaky neurons) (Figure 5F). In summary, these results demonstrate the distinct terminal arborizations of three C-type cutaneous afferents. Itch-sensing skin arbors, revealed using MrgprC11^{CreERT2} leaky neurons, are characterized by free endings with extensive axonal branching in the superficial epidermis and large receptive fields.

MrgprD^{CreERT2} leaky neurons exhibit limited expression of itch receptors

Since MrgprD mediates β-alanine-induced itch sensation, we asked if MrgprD^{CreERT2} leaky neurons also represent a subset of itch-sensing neurons. We examined the molecular feature of MrgprD^{CreERT2} leaky neurons from *MrgprD^{tdtomato}* mice (Figure 6A–H). All labeled neurons expressed MrgprD and most also expressed Lpar3 (75.3%), which is highly enriched in MrgprD$^+$ neurons (Figure 6A–B). However, none of them co-expressed with the

other examined itch receptors including MrgprA3, MrgprC11, Il31ra, and Htrf1. They do not express Nppb and very few co-expressed the histamine receptor Hrh1 (7%) (Figure 6C–H). Calcium imaging with sensory neurons isolated from *MrgprD^tdTomato; Pirt^GCaMP3* mice showed that a small percentage of MrgprD^{CreERT2} leaky neurons responded to β-alanine (8.5%). This is not a surprise since only half of MrgprD$^+$ neurons were reported to respond to β-alanine (Liu et al., 2012). 14.3% of the labeled neurons responded to LPA (Figure 5I–J). Only a few (0% – 4.7%) tdTomato$^+$ cells responded to other chemicals including chloroquine, Bam8–22, histamine, Il-31, LY344864, and capsaicin (Figure 6J). Therefore, MrgprD^{CreERT2} leaky neurons exhibit limited expression of itch receptors and weak response to pruritogens. These results suggest that MrgprD^{CreERT2} leaky neurons might represent a distinct population of pruriceptors involved in MrgprC11/A3-independent itch under normal and chronic itch conditions.

DISCUSSION

Our BAC (bacterial artificial chromosome) transgenic *MrgprC11^CreERT2* mouse line augments the limited availability of mouse line for studying Mrgprs family members. BAC transgenic mice have been serving as an invaluable tool for biomedical research in the past several decades (Heintz, 2001, Valjent et al., 2009). Since up to 300,000 base pairs of genomic segments can be carried by BAC construct, the intact necessary genetic sequences can be contained to allow the expression of the transgene in a spatially and temporally faithful manner. The methods developed to engineer the BAC DNA sequences further improves the value of BAC transgenic mice (Yang et al., 1997). In the current study, we have replaced the MrgprC11 sequence with CreERT2 recombinase in the BAC construct to generate *MrgprC11^CreERT2* line to achieve Cre-dependent reporter expression and neuronal tracing. Since BAC constructs randomly integrate into the genome, possibilities remain that essential genes may be disrupted or transgene expression may be affected by the regulatory elements surrounding the integration site. Therefore, screening and validation of multiple founder lines, which is time and labor consuming and might take months to years, normally are required for the successful generation of BAC transgenic lines. Despite this, we chose a BAC transgenic line instead of a knock-in mouse line. A knock-in *MrgprC11^CreERT2* line will have one copy of MrgprC11 sequence replaced by the CreERT2, and thus change the endogenous MrgprC11 expression, which might interfere with future studies investigation itch mechanisms. Our results showed that CreERT2 is faithfully expressed in MrgprC11$^+$ neurons, demonstrating that we have successfully generated the *MrgprC11^CreERT2* mouse line.

Results from our study and others demonstrate that MrgprA3$^+$ neurons and Nppb$^+$ neurons are two distinct itch-sensing neuronal populations with minimal overlap (Solinski et al., 2019). A common feature of itch-sensing neurons is that they are enriched with multiple itch receptors (Sharma et al., 2020, Solinski et al., 2019, Usoskin et al., 2015, Xing et al., 2020). MrgprA3$^+$ neurons express histamine receptors and two other identified itch receptors in the Mrgpr family: MrgprA1 and MrgprC11. Nppb$^+$ neurons are highly enriched with IL-31 receptors, Cysltr2, Htr1f, and S1pr1. The majority of MrgprC11^{CreERT2} leaky neurons we identified using sparse genetic labeling express markers for both itch-sensing populations including MrgprA3, MrgprC11, Hrh1, Nppb, IL31ra, Cysltr2, and Htr1f. Consistently,

calcium imaging analysis suggests that most MrgprC11^{CreERT2} leaky neurons respond to the corresponding pruritogens. This molecular feature suggests that these neurons likely represent the small overlapping piece of the MrgprA3$^+$ and Nppb$^+$ itch-sensing neurons. Indeed, activation of MrgprC11^{CreERT2} leaky neurons using a chemogenetic approach induced robust scratching behaviors, demonstrating that they are itch-sensing neurons. Therefore, the *MrgprC11^{CreERT2}* transgenic line we generated serves as a great genetic tool for the morphological characterization of itch-sensing neurons.

Sensory arbor morphology evolved to properly serve the physiological function of neurons. Our comparison of the peripheral arbors of MrgprC11^{CreERT2} leaky neurons, MrgprB4$^+$ neurons, and MrgprD^{CreERT2} leaky neurons highlights the diversity of the cutaneous C-type afferents. MrgprC11$^+$ itch-sensing arbors exhibit extensive axonal branching and free nerve endings in the superficial epidermis, suggesting that itch-sensing neurons are highly sensitive to pruritic stimuli on the surface of the skin. Circumferential-like endings associated with hair follicles were only occasionally observed in a small percentage of arbors (~10%), therefore they do not seem to be good candidates for mediating itch induced by hair vibration, a form of mechanically evoked itch (Fukuoka et al., 2013).

Sensory arbor area represents the receptive field size of sensory neurons. More than 10 morphologically distinct cutaneous arbor types have been characterized using sparse genetic labeling (Abraira and Ginty, 2013, Badea et al., 2012, Bai et al., 2015, Kuehn et al., 2019, Li and Ginty, 2014, Li et al., 2011, Rutlin et al., 2014, Wu et al., 2012) and the majority of them are large-diameter Aβ or Aδ fibers that are associated with specialized skin structure such as hairy follicles and merkel cells. Among them, the Aβ field LTMR innervating the hairy follicles exhibit a large receptive field (~ 3 mm^2) to detect gentle stroking across large fields of hairy skin (Bai et al., 2015). To our knowledge, four subtypes of free nerve endings have been identified: three subtypes reported here and by previous studies (Liu et al., 2007, Olson et al., 2017) and large area free ending (LA-FE) identified by random sparse labeling of *NFL^{CreERT2}* line (Wu et al., 2012). LA-FE arbors were named based on the morphological features and their function is unknown. They have the largest receptive fields among all reported (10–30 mm^2) with dense axonal branches uniformly distributed within the arbor (Wu et al., 2012). The area of itch-sensing neurons (1.60 ± 0.08 mm^2 in the dorsal hindpaw) is larger than the other two free ending arbors (MrgprB4$^+$ and MrgprD$^+$) and most of the non-free ending arbors. It is worth noting that the area of itch-sensing arbors may be slightly underestimated as only isolated arbors in the thoracic and lumbar regions were selected for analysis, whose sizes tend to be smaller than the overlapping ones. Interestingly, a study from human subjects suggests that itch-sensing neurons have large receptive fields. Schmelz et al. showed that a group of mechanically insensitive and histamine sensitive C-fiber, presumably itch-sensing, have much larger innervation territories (up to 45–88 mm diameter) than the histamine insensitive C fibers examined in human skin (Schmelz et al., 1997). This might explain why itch sensation is normally perceived as rising from a diffused large area instead of a focused spot.

It is well known that the morphology of cutaneous nerves can be profoundly changed by peripheral pathological conditions. Traditional analysis of intra-epidermal nerve fibers using skin sections have revealed morphological changes of fibers in a variety of dermatological

conditions (Kim T. W. et al., 2014, Nakamura et al., 2003, Taneda et al., 2011, Tsutsumi et al., 2016, Zhu et al., 2017). Recent work from Tan et al, combining immunostaining, optical clearing of whole skin samples, and confocal imaging, provided a more advanced 3-dimensional volumetric analysis of cutaneous nerves (Tan et al., 2019). This method offers the visualization of cutaneous nerve network in the epidermis and revealed intriguing results demonstrating the downregulation of epidermal innervation in pruritic atopic dermatitis and psoriasis skin. In our present study, the integration of genetic sparse labeling and axonal tracing allows us to examine the morphology of individual arbors of a specific itch-sensing neuronal population in mice. Future studies using this approach to examine changes under pathological conditions will provide insights into how itch-sensing arbors are modulated by the chronic itch conditions.

In summary, we generated a mouse line $MrgprC11^{CreERT2}$ that labels a subset of peptidergic itch-sensing neurons responding to multiple pruritogens. Using sparse genetic tracing, we characterized the itch-sensing arbors in the skin and demonstrated the morphological basis of itch detection.

MATERIAL AND METHODS

Animals

All experiments were performed with approval from the Georgia Institute of Technology Animal Use and Care Committee. $MrgprC11^{CreERT2}$ BAC transgenic line, $MrgprB4^{PLAP}$ knockin line (Liu et al., 2007), and $Pirt^{GCamp3}$ knockin line (Kim Y. S. et al., 2014) were generously provided by Dr. Xinzhong Dong at the Johns Hopkins University. $MrgprC11^{CreERT2}$ BAC transgenic mouse line was generated by the Gene Targeting & Transgenic Facility at Janelia Farm. $MrgprA3^{GFP-Cre}$ BAC transgenic line was generated by our previous study (Han et al., 2013). $MrgprD^{CreERT2}$ (Stock No: 031286), $ROSA26^{tdTomato}$ (Stock No: 007914), $ROSA26^{IAP}$ (Stock No: 009253), and $ROSA26^{DREADD}$ (Stock No: 026220) mouse lines were purchased from Jackson Laboratory. All the mice used had been backcrossed to C57BL/6 mice for at least ten generations. All the animals were housed in the vivarium with a 12-h light/dark cycle, and all the behavioral tests were performed from 9 a.m. to 1 p.m. in the light cycle. Mice were housed in groups, with a maximum of five per cage with food and water *ad libitum*.

PLAP whole-mount histochemistry staining

The procedure was performed as previously described (Liu et al., 2007). The tissues were cleared in BABB (Benzyl Alcohol and Benzyl Benzoate, 1:2 mixed together) before imaging on a ZEISS SteREO Discovery V12 stereomicroscope with a color camera. Two to five DRGs from one animal were used to quantify the number of PLAP$^+$ cells in DRGs collected from different body areas. For the quantification of the size of both skin arbors and central arbors, mice with similar age (P28 to P35) and body weight were used to avoid variation caused by animal size.

Immunohistochemistry staining and RNAscope *In situ* Hybridization

Immunohistochemistry staining was performed as previously described (Han et al., 2013). The following antibodies were used: rabbit anti-MrgprC11 (custom made by Proteintech groups, validated by previous study, 1:500) (Han et al., 2018), rabbit anti-TRPV1 (Novus, NBP1203487, 1:500), rat anti-Substance P (Millipore, MAB356, 1:500), goat anti-CGRP (BIO-RAD, 1720–9007, 1:500), conjugated IB4-Alexa 488 (Thermo Fisher, I-21411, 1:200), rabbit anti-P2X3 (Millipore, AB5898, 1:500), chicken anti-NF200 (Aves Labs, NFH877982, 1:500), rabbit anti-HA to detect hM3Dq expression (Cell Signaling Technologies, 3724S, 1:500), donkey anti-rabbit Alexa Fluor 488 (Thermo Fisher, A11056), goat anti-chicken Alexa Fluor 488 (Thermo Fisher, A21127), donkey anti-goat Alexa Fluor 488 (Thermo Fisher, A21206), donkey anti-goat Alexa Fluor 546 (Thermo Fisher, A31572), and donkey anti-rat Alexa Fluor 488 (Thermo Fisher, A11039). All secondary antibodies were used at 1:500 dilution. To induce tdtomato expression in all MrgprC11$^+$ neurons, *MrgprC11^{tdTomato}* mice were treated daily via oral gavage (22g × 25mm, FTP-22–25, Instech Laboratories) with 100 mg/kg of tamoxifen (T5648, Sigma) dissolved in sunflower seed oil (S5007, Sigma) at P14-P18. To directly visualize MrgprC11$^+$ nerves in the skin sections, cross skin sections from tamoxifen-treated *MrgprC11^{tdTomato}* mice were collected and tdTomato$^+$ nerves were directly imaged with Confocal Microscopy.

RNAscope *in situ* hybridization was performed using the RNAscope fluorescent multiplex kit (ACD Cat#320850) according to the manufacturer's instructions. The following probes were used: tdTomato (317041), MrgprA3 (548161), MrgprC11 (488771), MrgprD (417921), Hrh1 (491141), Il31ra (418411), Htrf1 (315881), Nppb (425021), Nmb (459931), Lpar3 (432591).

Quantification results for every marker were collected from 4–12 lumbar DRGs dissected from 3 adult mice.

Behavioral tests

The experiments were performed as previously described (Xing et al., 2020). Briefly, Clozapine N-oxide (CNO 16882, Cayman, 10 mg/kg, 100 μl) were injected subcutaneously into the nape of the neck. Behavioral responses were video recorded and analyzed by experimenters blind to genotype.

Calcium Imaging

Calcium imaging was performed with sensory neurons collected from *MrgprC11^{tdTomato}; Pirt^{GCaMP3}* mice or *MrgprD^{tdTomato}; Pirt^{GCaMP3}* mice. Three *MrgprC11^{tdTomato}; Pirt^{GCaMP3}* mice and two *MrgprD^{tdTomato}; Pirt^{GCaMP3}* mice were used for calcium imaging and quantification. A 20% increase in GCaMP3 fluorescence intensity was set as the threshold to identify responding cells. Chemicals used are listed as follows: chloroquine (Sigma PHR1258), Bam8–22 (custom synthesized by Genscript), histamine (Sigma H7250), IL-31 (R&D 3028-ML-010), LY344864 (Sigma SML0556), β-alanine (Sigma 146064), Capsaicin (Sigma M2028), LPA 18:1 (Sigma 857130).

ACKNOWLEDGMENTS

Reference

Abraira VE, Ginty DD. The sensory neurons of touch. Neuron 2013;79(4):618–39. [PubMed: 23972592]

Badea TC, Williams J, Smallwood P, Shi M, Motajo O, Nathans J. Combinatorial expression of Brn3 transcription factors in somatosensory neurons: genetic and morphologic analysis. J Neurosci 2012;32(3):995–1007. [PubMed: 22262898]

Bai L, Lehnert BP, Liu J, Neubarth NL, Dickendesher TL, Nwe PH, et al. Genetic Identification of an Expansive Mechanoreceptor Sensitive to Skin Stroking. Cell 2015;163(7):1783–95. [PubMed: 26687362]

Basbaum AI, Bautista DM, Scherrer G, Julius D. Cellular and molecular mechanisms of pain. Cell 2009;139(2):267–84. [PubMed: 19837031]

Crawford LK, Caterina MJ. Functional Anatomy of the Sensory Nervous System: Updates From the Neuroscience Bench. Toxicologic pathology 2020;48(1):174–89. [PubMed: 31554486]

Fukuoka M, Miyachi Y, Ikoma A. Mechanically evoked itch in humans. Pain 2013;154(6):897–904. [PubMed: 23582153]

Ghitani N, Barik A, Szczot M, Thompson JH, Li C, Le Pichon CE, et al. Specialized Mechanosensory Nociceptors Mediating Rapid Responses to Hair Pull. Neuron 2017;95(4):944–54 e4. [PubMed: 28817806]

Han L, Limjunyawong N, Ru F, Li Z, Hall OJ, Steele H, et al. Mrgprs on vagal sensory neurons contribute to bronchoconstriction and airway hyper-responsiveness. Nat Neurosci 2018;21(3):324–8. [PubMed: 29403029]

Han L, Ma C, Liu Q, Weng HJ, Cui Y, Tang Z, et al. A subpopulation of nociceptors specifically linked to itch. Nat Neurosci 2013;16(2):174–82. [PubMed: 23263443]

Hans S, Kaslin J, Freudenreich D, Brand M. Temporally-controlled site-specific recombination in zebrafish. PLoS One 2009;4(2):e4640. [PubMed: 19247481]

Heintz N BAC to the future: the use of bac transgenic mice for neuroscience research. Nat Rev Neurosci 2001;2(12):861–70. [PubMed: 11733793]

Hooijkaas AI, Gadiot J, van der Valk M, Mooi WJ, Blank CU. Targeting BRAFV600E in an inducible murine model of melanoma. The American journal of pathology 2012;181(3):785–94. [PubMed: 22796458]

Ikoma A, Steinhoff M, Stander S, Yosipovitch G, Schmelz M. The neurobiology of itch. Nat Rev Neurosci 2006;7(7):535–47. [PubMed: 16791143]

Kim TW, Shim WH, Kim JM, Mun JH, Song M, Kim HS, et al. Clinical characteristics of pruritus in patients with scalp psoriasis and their relation with intraepidermal nerve fiber density. Annals of dermatology 2014;26(6):727–32. [PubMed: 25473225]

Kim YS, Chu Y, Han L, Li M, Li Z, LaVinka PC, et al. Central terminal sensitization of TRPV1 by descending serotonergic facilitation modulates chronic pain. Neuron 2014;81(4):873–87. [PubMed: 24462040]

Kuehn ED, Meltzer S, Abraira VE, Ho CY, Ginty DD. Tiling and somatotopic alignment of mammalian low-threshold mechanoreceptors. Proc Natl Acad Sci U S A 2019;116(19):9168–77. [PubMed: 30996124]

Li L, Ginty DD. The structure and organization of lanceolate mechanosensory complexes at mouse hair follicles. Elife 2014;3:e01901. [PubMed: 24569481]

Li L, Rutlin M, Abraira VE, Cassidy C, Kus L, Gong S, et al. The functional organization of cutaneous low-threshold mechanosensory neurons. Cell 2011;147(7):1615–27. [PubMed: 22196735]

Liu Q, Sikand P, Ma C, Tang Z, Han L, Li Z, et al. Mechanisms of itch evoked by beta-alanine. J Neurosci 2012;32(42):14532–7. [PubMed: 23077038]

Liu Q, Tang Z, Surdenikova L, Kim S, Patel KN, Kim A, et al. Sensory neuron-specific GPCR Mrgprs are itch receptors mediating chloroquine-induced pruritus. Cell 2009;139(7):1353–65. [PubMed: 20004959]

Liu Q, Vrontou S, Rice FL, Zylka MJ, Dong X, Anderson DJ. Molecular genetic visualization of a rare subset of unmyelinated sensory neurons that may detect gentle touch. Nat Neurosci 2007;10(8):946–8. [PubMed: 17618277]

Liu Q, Weng HJ, Patel KN, Tang Z, Bai H, Steinhoff M, et al. The distinct roles of two GPCRs, MrgprC11 and PAR2, in itch and hyperalgesia. Sci Signal 2011;4(181):ra45. [PubMed: 21775281]

Nakamura M, Toyoda M, Morohashi M. Pruritogenic mediators in psoriasis vulgaris: comparative evaluation of itch-associated cutaneous factors. The British journal of dermatology 2003;149(4):718–30. [PubMed: 14616362]

Olson W, Abdus-Saboor I, Cui L, Burdge J, Raabe T, Ma M, et al. Sparse genetic tracing reveals regionally specific functional organization of mammalian nociceptors. Elife 2017;6.

Olson W, Luo W. Somatotopic organization of central arbors from nociceptive afferents develops independently of their intact peripheral target innervation. The Journal of comparative neurology 2018;526(18):3058–65. [PubMed: 30225912]

Reddy VB, Sun S, Azimi E, Elmariah SB, Dong X, Lerner EA. Redefining the concept of protease-activated receptors: cathepsin S evokes itch via activation of Mrgprs. Nat Commun 2015;6:7864. [PubMed: 26216096]

Rutlin M, Ho CY, Abraira VE, Cassidy C, Bai L, Woodbury CJ, et al. The cellular and molecular basis of direction selectivity of Adelta-LTMRs. Cell 2014;159(7):1640–51. [PubMed: 25525881]

Scheibel ME, Scheibel AB. Terminal axonal patterns in cat spinal cord. II. The dorsal horn. Brain Res 1968;9(1):32–58. [PubMed: 5699822]

Schmelz M, Schmidt R, Bickel A, Handwerker HO, Torebjork HE. Specific C-receptors for itch in human skin. J Neurosci 1997;17(20):8003–8. [PubMed: 9315918]

Sharif B, Ase AR, Ribeiro-da-Silva A, Seguela P. Differential Coding of Itch and Pain by a Subpopulation of Primary Afferent Neurons. Neuron 2020;106(6):940–51 e4. [PubMed: 32298640]

Sharma N, Flaherty K, Lezgiyeva K, Wagner DE, Klein AM, Ginty DD. The emergence of transcriptional identity in somatosensory neurons. Nature 2020;577(7790):392–8. [PubMed: 31915380]

Solinski HJ, Kriegbaum MC, Tseng PY, Earnest TW, Gu X, Barik A, et al. Nppb Neurons Are Sensors of Mast Cell-Induced Itch. Cell Rep 2019;26(13):3561–73 e4. [PubMed: 30917312]

Stone JS, Wisner SR, Bucks SA, Mellado Lagarde MM, Cox BC. Characterization of Adult Vestibular Organs in 11 CreER Mouse Lines. Journal of the Association for Research in Otolaryngology : JARO 2018;19(4):381–99. [PubMed: 29869046]

Sugiura Y, Lee CL, Perl ER. Central projections of identified, unmyelinated (C) afferent fibers innervating mammalian skin. Science 1986;234(4774):358–61. [PubMed: 3764416]

Sugiura Y, Terui N, Hosoya Y. Difference in distribution of central terminals between visceral and somatic unmyelinated (C) primary afferent fibers. Journal of neurophysiology 1989;62(4):834–40. [PubMed: 2809705]

Tan Y, Ng WJ, Lee SZX, Lee BTK, Nattkemper LA, Yosipovitch G, et al. 3-Dimensional Optical Clearing and Imaging of Pruritic Atopic Dermatitis and Psoriasis Skin Reveals Downregulation of Epidermal Innervation. J Invest Dermatol 2019;139(5):1201–4. [PubMed: 30471253]

Taneda K, Tominaga M, Negi O, Tengara S, Kamo A, Ogawa H, et al. Evaluation of epidermal nerve density and opioid receptor levels in psoriatic itch. The British journal of dermatology 2011;165(2):277–84. [PubMed: 21457210]

Tsutsumi M, Kitahata H, Fukuda M, Kumamoto J, Goto M, Denda S, et al. Numerical and comparative three-dimensional structural analysis of peripheral nerve fibres in epidermis of patients with atopic dermatitis. The British journal of dermatology 2016;174(1):191–4. [PubMed: 26114666]

Usoskin D, Furlan A, Islam S, Abdo H, Lonnerberg P, Lou D, et al. Unbiased classification of sensory neuron types by large-scale single-cell RNA sequencing. Nat Neurosci 2015;18(1):145–53. [PubMed: 25420068]

Valjent E, Bertran-Gonzalez J, Herve D, Fisone G, Girault JA. Looking BAC at striatal signaling: cell-specific analysis in new transgenic mice. Trends Neurosci 2009;32(10):538–47. [PubMed: 19765834]

Wan L, Jin H, Liu XY, Jeffry J, Barry DM, Shen KF, et al. Distinct roles of NMB and GRP in itch transmission. Sci Rep 2017;7(1):15466. [PubMed: 29133874]

Wu H, Williams J, Nathans J. Morphologic diversity of cutaneous sensory afferents revealed by genetically directed sparse labeling. Elife 2012;1:e00181. [PubMed: 23256042]

Xing Y, Chen J, Hilley H, Steele H, Yang J, Han L. Molecular signature of pruriceptive MrgprA3(+) neurons. J Invest Dermatol 2020.

Yang XW, Model P, Heintz N. Homologous recombination based modification in Escherichia coli and germline transmission in transgenic mice of a bacterial artificial chromosome. Nature biotechnology 1997;15(9):859–65.

Zhu Y, Hanson CE, Liu Q, Han L. Mrgprs activation is required for chronic itch conditions in mice. Itch (Phila) 2017;2(3).

Zylka MJ, Rice FL, Anderson DJ. Topographically distinct epidermal nociceptive circuits revealed by axonal tracers targeted to Mrgprd. Neuron 2005;45(1):17–25. [PubMed: 15629699]
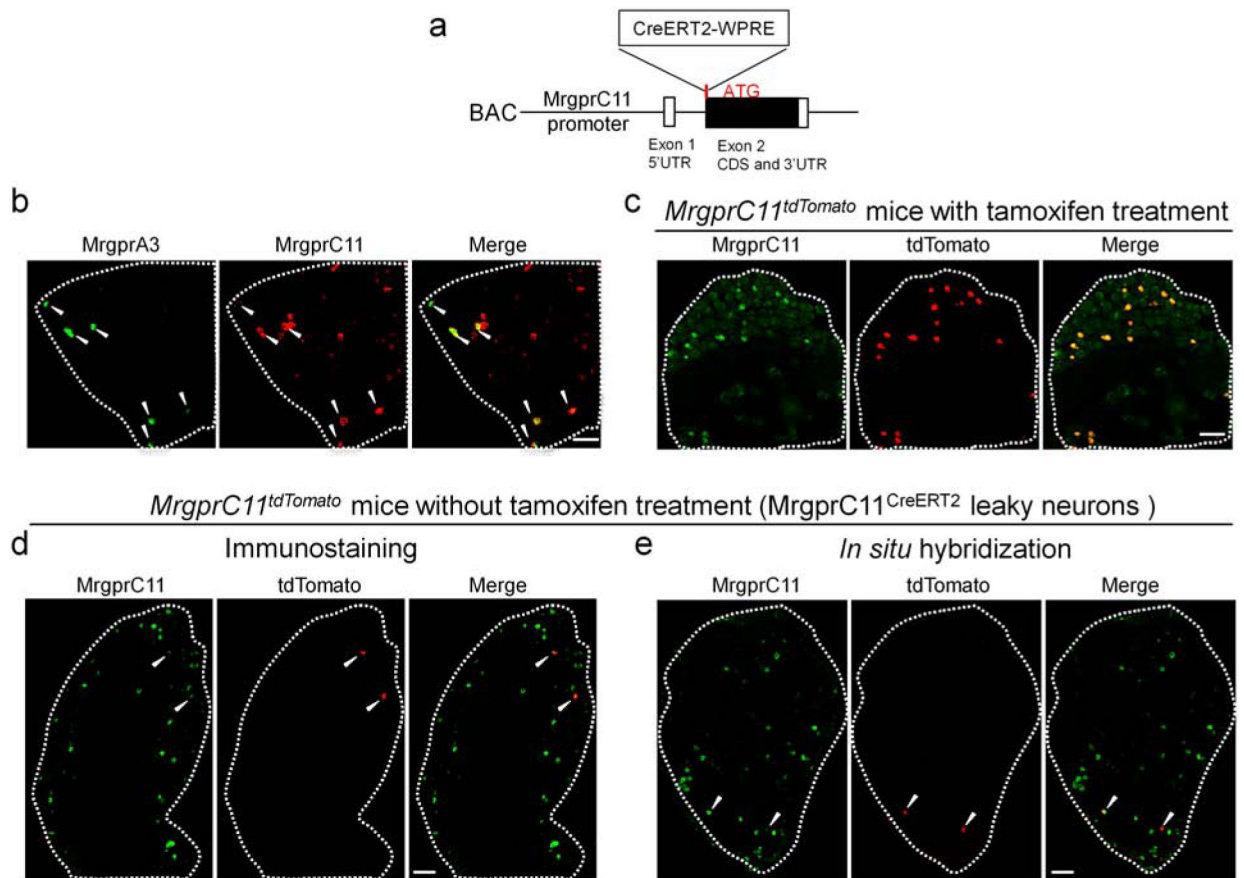
Figure 1. Generation of *MrgprC11^CreERT2* BAC transgenic mouse line
(A) Diagram showing the design of the BAC construct. CreERT2 sequence was inserted right after the ATG of MrgprC11 in the second exon. Woodchuck Hepatitis Virus Posttranscriptional Regulatory Element (WPRE), a sequence commonly used to improve transgene expression, was added after CreERT2. CDS: coding sequence. UTR: untranslated region. (B) Lumbar DRG sections from *MrgprA3^GFP-Cre* mice stained with GFP and MrgprC11 antibody. MrgprA3$^+$ neurons are labeled by GFP expression. (C) L3-L5 DRG sections from tamoxifen-treated *MrgprC11^tdTomato* mice labeled with MrgprC11 antibody (green). tdTomato (red) is faithfully expressed in MrgprC11$^+$ DRG neurons. (D-E) Immunostaining (D) and RNAscope *in situ* hybridization (E) of lumbar DRG sections from *MrgprC11^tdTomato* mice without tamoxifen treatment showing co-expression of MrgprC11 and tdTomato. Scale bars = 100 μm.
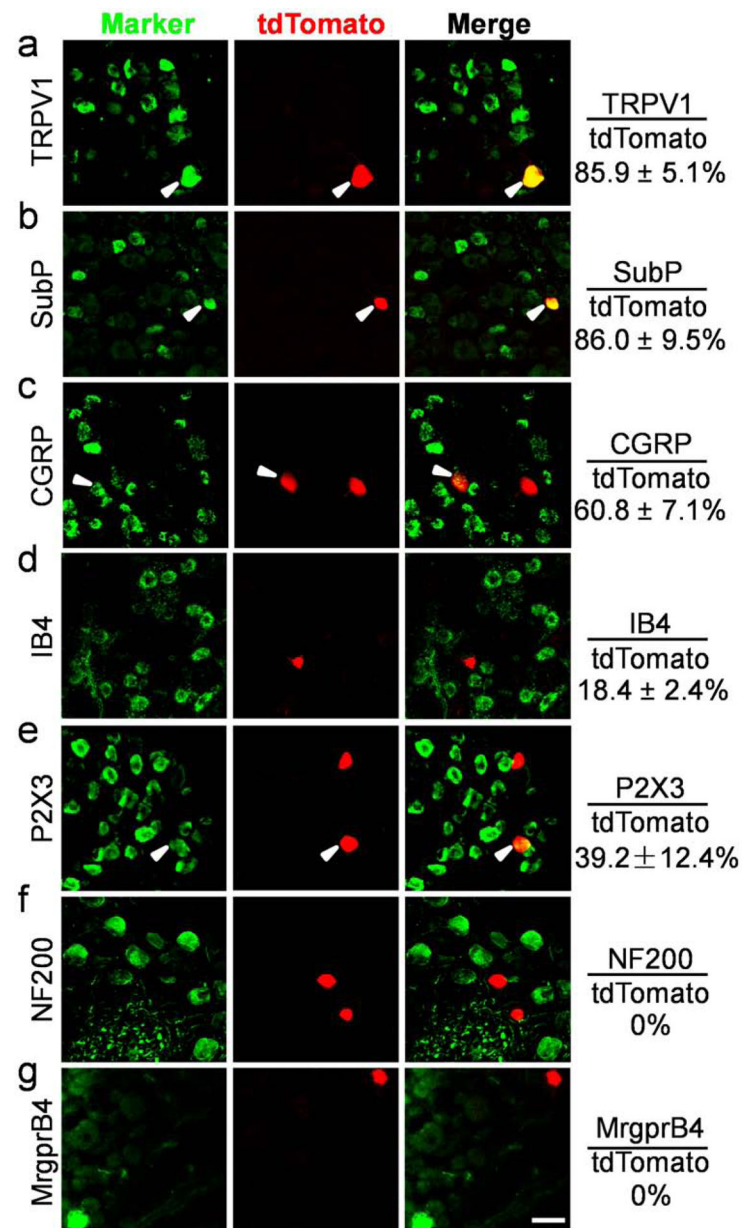
Figure 2. MrgprC11^{CreERT2} leaky neurons label a small subset of peptidergic nociceptors.
(A-G) Double immunostaining of lumbar DRG sections from *MrgprC11^{tdTomato}* mice without tamoxifen treatment to detect indicated sensory neuron markers in *MrgprC11^{CreERT2}* leaky neurons. Overlap quantifications were shown on the right of each panel (% of tdTomato$^+$ cells that express markers). Arrowheads point to overlapping cells. Scale bars = 50 μm. N = 3 mice for each marker.
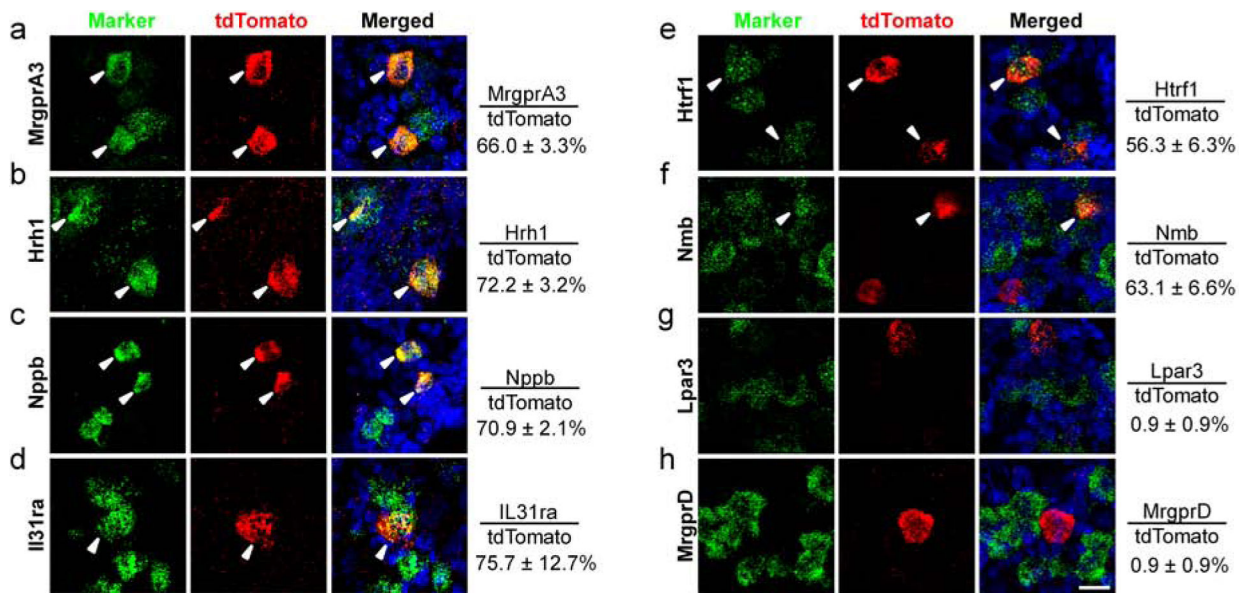
Figure 3. MrgprC11^CreERT2 leaky neurons express multiple itch receptors.
(A-H) RNAscope fluorescent *in situ* hybridization detecting itch-related molecules using lumbar DRG sections from *MrgprC11^tdTomato* mice. Overlap quantifications were shown on the right of each panel (% of tdTomato+ cells that express markers). Arrowheads point to overlapping cells. Scale bars = 25 μm. N = 3 mice for each marker.
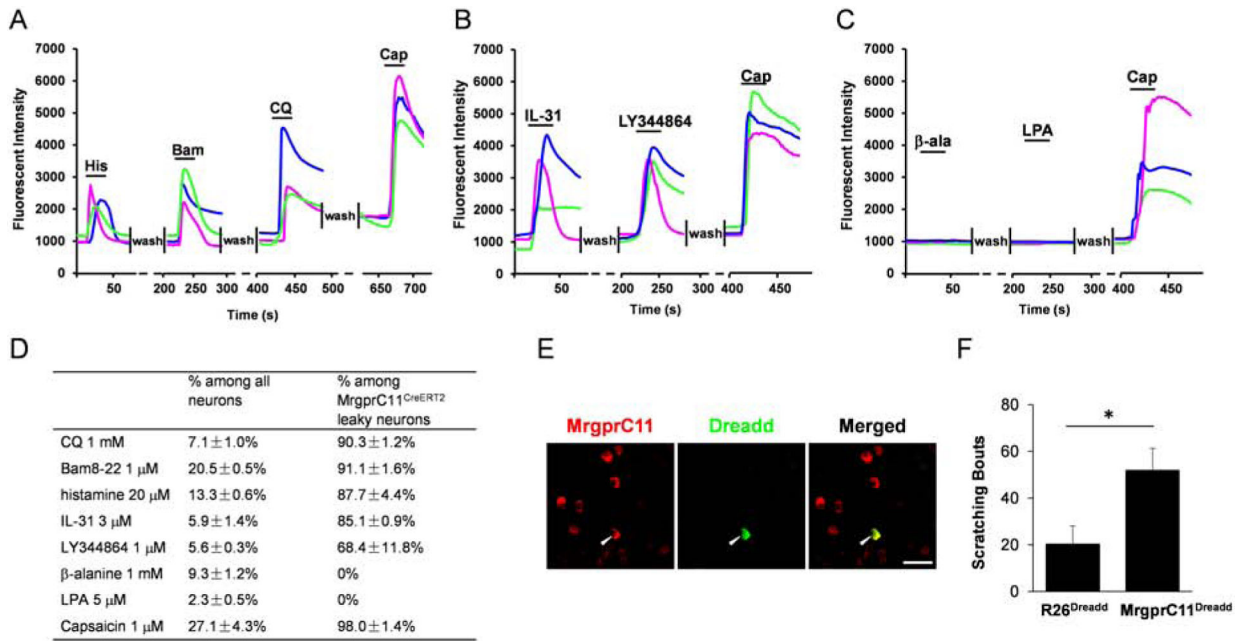
	% among all neurons	% among MrgprC11[CreERT2] leaky neurons
CQ 1 mM	7.1±1.0%	90.3±1.2%
Bam8-22 1 μM	20.5±0.5%	91.1±1.6%
histamine 20 μM	13.3±0.6%	87.7±4.4%
IL-31 3 μM	5.9±1.4%	85.1±0.9%
LY344864 1 μM	5.6±0.3%	68.4±11.8%
β-alanine 1 mM	9.3±1.2%	0%
LPA 5 μM	2.3±0.5%	0%
Capsaicin 1 μM	27.1±4.3%	98.0±1.4%

Figure 4. MrgprC11[CreERT2] leaky neurons represent itch-sensing neurons.

(A-C) Representative traces evoked by different pruritogens in cultured DRG sensory neurons isolated from the *MrgprC11[tdtomato]; Pirt[GCaMP3]* mice. (D) Table showing the concentration of pruritogens tested (left column), the percentages of responding neurons among all cells (middle column), and the percentages of responding neurons among MrgprC11[CreERT2] leaky cells (right column). N = 3 mice for each pruritogen. (E) Double immunostaining of lumbar DRG sections collected from *MrgprC11[DREADD]* mice using MrgprC11 and GFP antibodies. The hM3Dq transgene in *ROSA26[DREADD]* mice was fused with mCitrine that can be detected by GFP antibody to examine the expression of DREADD in MrgprC11^{+} neurons. Scale bars = 50 μm. (F) Subcutaneous injection of CNO (10 mM) into the nape of the neck induced significant scratching behavior in *MrgprC11[DREADD]* mice compared to *R26[DREADD]* mice. N = 8 for the *MrgprC11[DREADD]* group and N = 6 for the R26[DREADD] group. *P < 0.05. Two-tailed unpaired Student's t test. Error bars represent s.e.m.
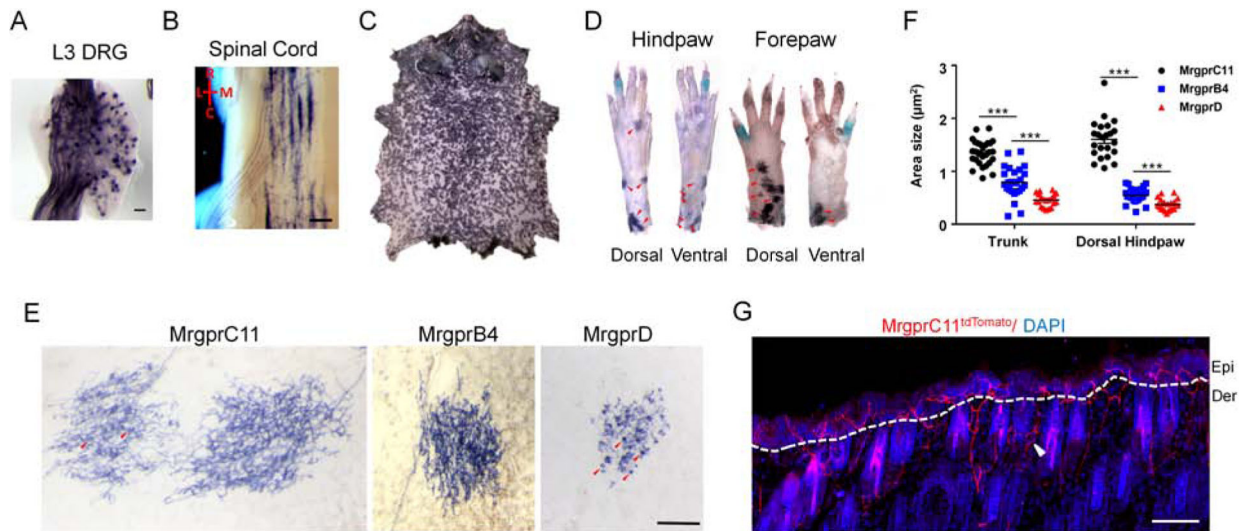
Figure 5. Itch-sensing skin arbors exhibit free nerve endings in the superficial epidermis, dense axon density, and large receptive fields.

(A-D) Whole-mount PLAP histochemistry staining of a lumbar level 3 (L3) DRG (A), spinal cord (B), whole body skin (C), and the distal limbs (D) from *MrgprC11^{IAP}* mouse. (A) Approximately 1% of DRG sensory neurons were labeled by the axonal tracer PLAP. (B) Central arbors of MrgprC11^{CreERT2} leaky neurons. R: rostral, C: caudal, L: lateral, M: medial. (C) Whole body skin showing the distribution of MrgprC11$^+$ skin arbor. (D) Distribution of MrgprC11$^+$ arbor on distal limbs. Arbors, indicated by the red arrows, were observed in the dorsal hairy skin of the paws, not in the ventral plantar glabrous skin. Multiple high magnification images were stitched together to show the whole paws. (E) High magnification images showing single skin arbor morphology using *MrgprC11^{IAP}, MrgprB4^{PLAP}, and MrgprD^{IAP}* mice. Circumferential-like endings associated with hair follicles were observed frequently in almost every MrgprD$^+$ arbors and occasionally in MrgprC11$^+$ arbors. Some of them are indicated with red arrowheads. Two neighboring MrgprC11$^+$ arbors were shown with one of them exhibiting several circumferential-like endings. Scale bars = 500 μm. (F) Areas of the three subtypes of nociceptive skin arbors in the trunk and dorsal hindpaw. Data present as mean ± s.e.m. (G) Skin cross-section from the trunk area of tamoxifen-treated *MrgprC11^{tdTomato}* mouse. MrgprC11$^+$ nerves are free nerve endings penetrating into the superficial layers of the epidermis. Nerves wrapping around the hair follicles, indicated by the white arrowhead, were occasionally observed. Scale bars = 50 μm in A, E and G, 100 μm in B.
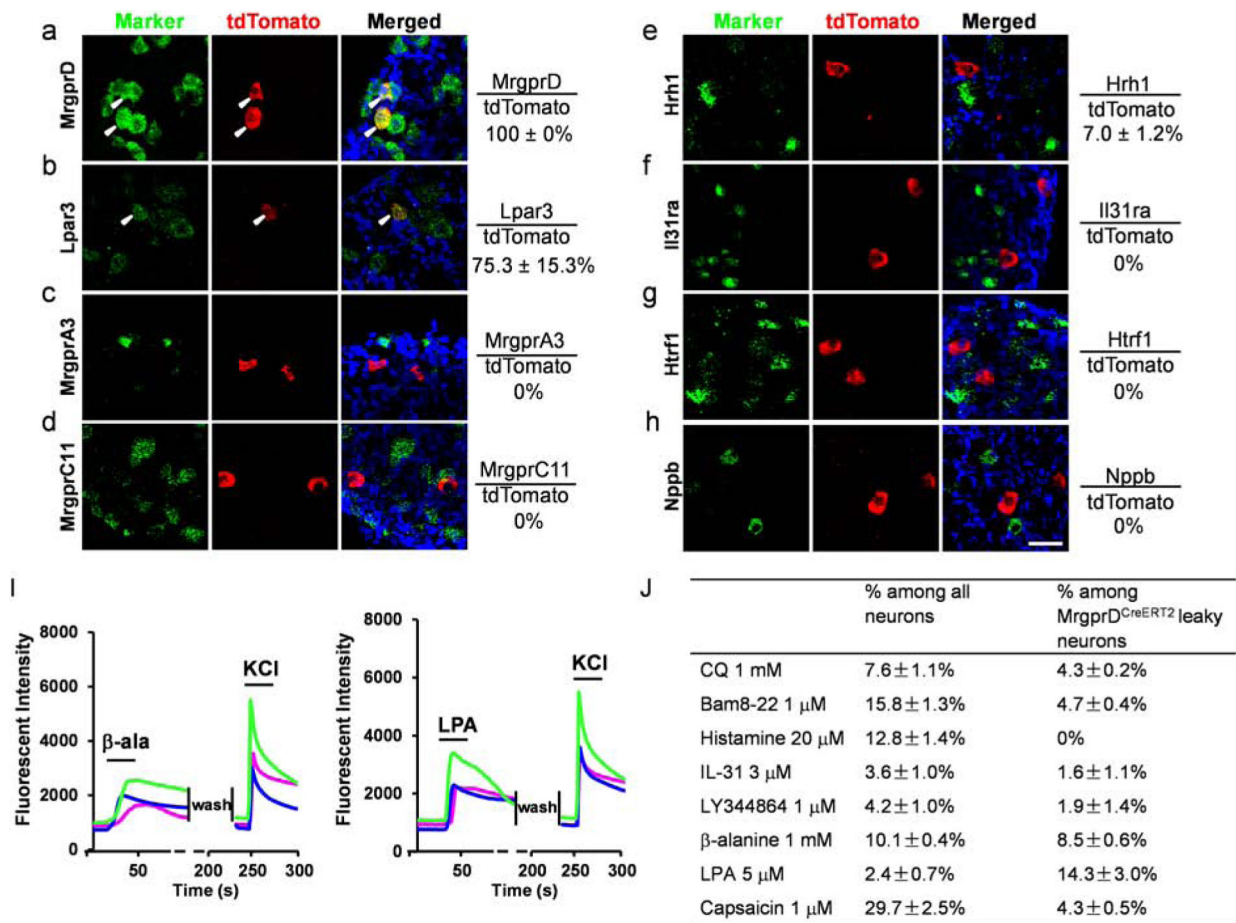
Figure 6. MrgprD^CreERT2 leaky neurons express limited itch receptors.

(A-H) RNAscope fluorescent *in situ* hybridization detecting itch-related molecules using lumbar DRG sections from *MrgprD^tdTomato* mice. Overlap quantifications were shown on the right of each panel (% of tdTomato+ cells that express markers). Arrowheads point to overlapping cells. Scale bars = 50 μm. N = 3 mice for each marker. (I) Representative traces evoked by different pruritogens in cultured DRG sensory neurons isolated from the *MrgprD^tdtomato; Pirt^GCaMP3* mice. A small percentage of MrgprD^CreERT2 leaky neurons responded to β-alanine and LPA. All cells were subjected to KCl (50 mM) treatment to verify their neuronal identity. (J) Table showing the concentration of pruritogens tested (left column), the percentages of responding neurons among all cells (middle column), and the percentages of responding neurons among MrgprD^CreERT2 leaky cells (right column). N = 2 mice for each pruritogen.